

## Observations of light-induced structural changes of retinal within rhodopsin

GERHARD GRÖBNER\*, IAN BURNETT, CLEMENS GLAUBITZ,  
GREGORY HOI†, A. JAMES MASON & ANTHONY WATTS

Biomembrane Structure Unit, Department of Biochemistry, University of Oxford, South Parks Road, Oxford OX1 3QU, UK

\*Present address: Department of Chemistry, Biophysical Chemistry, Umeå University, SE-901 87 Umeå, Sweden.

†Present address: University of Connecticut, Molecular & Cell Biology, LSA 205, 75 North Eagleville Road, U-125 Storrs, Connecticut 06269-3125, USA.

Correspondence and requests for materials should be addressed to A.W. (e-mail: awatts@bioch.ox.ac.uk). The structural data for the chromophore can be obtained from the authors and will be posted at <http://www.bioch.ox.ac.uk/~watts>.

**Photo-isomerization of the 11-*cis* retinal chromophore activates the mammalian light-receptor rhodopsin<sup>1</sup>, a representative member of a major superfamily of transmembrane G-protein-coupled receptor proteins (GPCRs) responsible for many cell signal communication pathways. Although low-resolution (5Å) electron microscopy studies<sup>2, 3</sup> confirm a seven transmembrane helix bundle as a principal structural component of rhodopsin, the structure of the retinal within this helical bundle is not known in detail. Such information is essential for any theoretical or functional understanding of one of the fastest occurring photoactivation processes in nature, as well as the general mechanism behind GPCR activation<sup>4-6</sup>. Here we determine the three-dimensional structure of 11-*cis* retinal bound to bovine rhodopsin in the ground state at atomic level using a new high-resolution solid-state NMR method<sup>7</sup>. Significant structural changes are observed in the retinal following activation by light to the photo-activated MI state of rhodopsin giving the all-*trans* isomer of the chromophore. These changes are linked directly to the activation of the receptor, providing an insight into the activation mechanism of this class of receptors at a molecular level.**

In the mammalian photoreceptor rhodopsin, the external stimulus is an optical one and it controls the activation of a GTP-protein-coupled signal transduction pathway leading to a neural response<sup>1</sup>. More usually, however, GPCRs transmit chemical (hormone, pharmaceutically mediated) signals across cellular membranes<sup>4, 8</sup>. Even though GPCRs share a putative common spatial protein arrangement<sup>4, 5</sup>, no member of this family, other than rhodopsin<sup>2-6</sup>, has yet been resolved in any significant (<5Å) structural detail, which explains its importance in any structural and functional studies

for the whole family of GPCRs to reveal their putative common mechanism of activation. The lack of high-resolution ( $<5\text{\AA}$ ) structural information for rhodopsin means that no comprehensive structural description at the molecular level is available for 11-*cis* retinal, the light sensitive prosthetic group of rhodopsin whose interaction with its receptor binding pocket causes rhodopsin activation. The conjugated polyene chain of retinal and its five methyl groups and cyclohexene ring (Fig. 1) all interact with various amino acids of the retinal binding pocket, and so may also induce conformational changes within the protein upon light-induced isomerization. Also, the seven-helix bundle arrangement of the protein undergoes a conformational change to activate the GTP-protein transducin<sup>9</sup> followed by a cascade of signalling events. Numerous biophysical studies have provided a significant body of indirect and often inconsistent evidence for the retinal environment without resolving the molecular detail of either the retinal binding site or the retinal conformation itself, or the structural features of the molecular mechanism of light activation<sup>1, 2, 9-14</sup>. More recently, solid state NMR studies have provided some direct and highly localized details of the Schiff base environment and the non-planarity in the polyene chain<sup>14-18</sup>. However, a complete picture of the structure and orientation of retinal at an atomic level has still not emerged, and information essential for any theoretical and functional understanding of the general mechanism behind rhodopsin activation is far from complete.

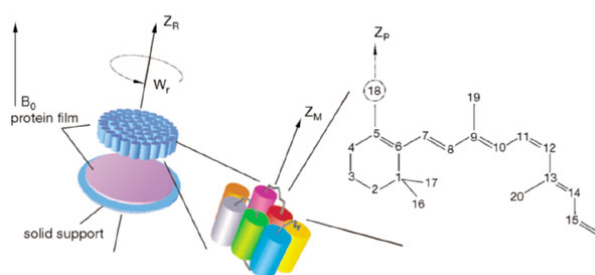


**Figure 1** In the magic angle oriented sample spinning (MAOSS) NMR approach used here, uni-axially oriented phospholipid membranes containing bovine rhodopsin were stacked on glass plates in a MAS rotor, with rotor axis  $Z_R$  parallel to the sample director.□

To determine the three-dimensional structure and alignment of retinal in the binding pocket of rhodopsin at the atomic level, high-resolution solid state deuterium ( $^2\text{H}$ ) NMR methods were employed, namely static<sup>19, 20</sup> and the newly developed magic angle oriented sample spinning (MAOSS) approach<sup>7</sup>. The suggested 11-*cis* retinal structure in the ground state of the receptor is distorted<sup>17</sup>, with the ring moiety twisted against the polyene chain and further twists around the  $\text{C}_{10}=\text{C}_{11}$  double bond. Therefore, we synthesized three different retinals<sup>7, 20</sup>, which are all analogues of the naturally occurring chromophore but with each of the following methyl groups,  $\text{C}_5-\text{C}_{18}$ ,  $\text{C}_9-\text{C}_{19}$  and  $\text{C}_{13}-\text{C}_{20}$ , carrying deuterium  $\text{C}-\text{C}(^2\text{H})_3$ , to be used separately as non-perturbing NMR reporters of molecular structure. The solid state NMR spectra recorded from each of the labelled retinals in rhodopsin contain direct information about the orientation of the labelled  $\text{C}-\text{C}(^2\text{H})_3$  bond with respect to the applied magnetic field<sup>7, 20</sup> and directly reveal the orientational constraints for each of the various molecular segments of the chromophore within the protein and the changes induced after isomerization by light.

Representative  $^2\text{H}$  MAOSS NMR spectra are shown in Fig. 2a and b for rhodopsin containing a  $\text{C}_5-\text{C}_{18}(^2\text{H})_3$  group on the cyclohexene ring of the retinal, in the ground state and upon photo-activation in its thermally trapped MI state. Each sideband

intensity is a function of size and orientation of the deuterium quadrupolar coupling tensor, allowing a precise, direct and reliable measurement of the C–C(2H) 3 bond vector orientation to be made, as illustrated with the root-mean-square deviation plots of the C5–C18(2H) 3 orientation with respect to the membrane normal. In this way a comprehensive analysis provides information not only about the orientation of the chromophore in the binding pocket of rhodopsin, but also about the intramolecular changes occurring upon photo-activation in the MI state. Significant changes in the bond vectors are observed upon photo-excitation of retinal within rhodopsin, in particular in the ring moiety where the C5–C18 bond has an orientation of  $21 \pm 5^\circ$  in the inactivated state with respect to the membrane normal, changing markedly to  $62 \pm 7^\circ$  for the MI state (Table 1), this being the intermediate immediately before major protein conformational changes occur.

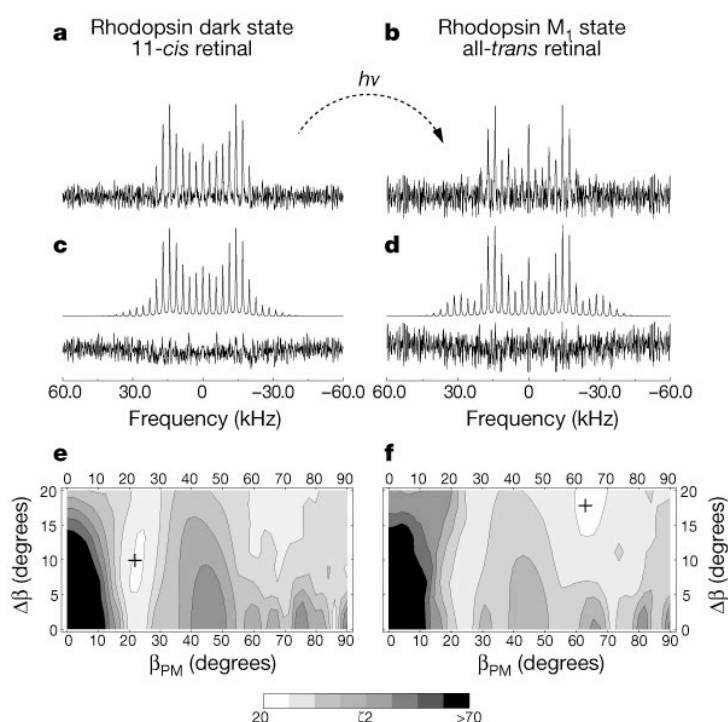


**Figure 2** Deuterium-MAOSS NMR spectra of [18-C(2H)3]-retinal in dark adapted rhodopsin (a) and upon photo-activation in the MI state (illuminated below 273K) (b), at  $\nu = 2860$  MHz and  $T = 213$  K.

The detailed intramolecular structural information obtained for retinal within the protein is resolved without the need to rely on any knowledge of the protein structure itself. In particular, details can be resolved for the orientation of the ring moiety of retinal, and its twist relative to the conjugated polyene chain, a topic which has been the centre of much debate substantiated mainly by studies using various optical absorption and  $^{13}\text{C}$ -NMR chemical shift data<sup>10, 11, 21</sup>, even though a complete description of the chromophore was not available. Here, the MAOSS approach provides tight constraints (bond vectors for C–C(2H)3 determined to  $5\text{--}7^\circ$ ) on the orientation of the ring moiety in the protein body and its twist relative to the other individual molecular segments. From static  $^2\text{H}$  NMR<sup>19</sup>, the orientational constraints for the C19 methyl group are  $44 \pm 5^\circ$  and for the C20 group are  $30 \pm 5^\circ$ . Using these direct orientational constraints, and the torsional and distance constraints measured by solid-state NMR for the C10–C11–C12–C13 segment<sup>16–18</sup>, we have constructed the first complete high-resolution, three-dimensional structure of the orientation and conformation of 11-*cis* retinal in the binding pocket of rhodopsin (Fig. 3).

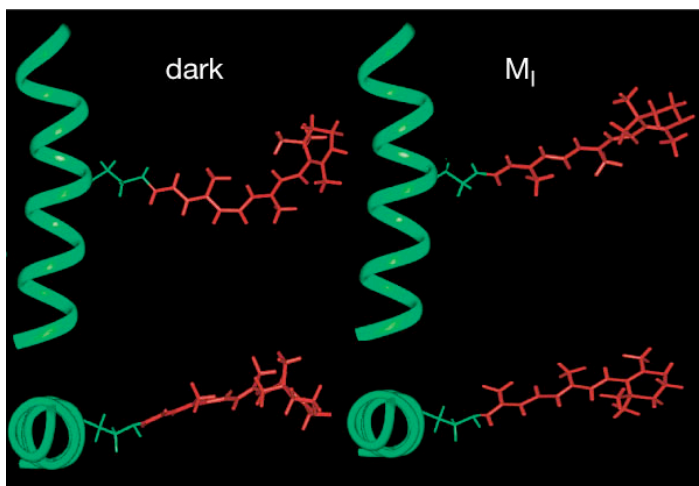


**Figure 3** The structure and orientation of the chromophore 11-*cis* retinal in the binding pocket of the GPCR protein bovine rhodopsin in its dark-adapted ground state (left), including the experimentally obtained structural constraints (helix 7 of the protein used as z-axis reference; helix only partially displayed). □

Major differences are observed for the position of the cyclohexene ring with respect to the polyene chain when compared with earlier suggested structural models<sup>10, 13, 14, 21</sup>. To accommodate the tilt angle of  $21.5^\circ$  obtained here for the C5–C18 bond vector, a rotational movement of the ring must be performed around the C6–C7 bond axis, which itself is tilted by  $50^\circ$  from the protein long axis. This procedure results in two possible positions of the ring, with either a twist of  $28^\circ$  around the C6–C7 axis or of  $70^\circ$  (corresponding to a torsion angle of  $-28^\circ$  and  $-70^\circ$  for the C1–C6–C7–C8 segment). The latter (shown in Fig. 3) being an angle which is more likely to reduce steric interaction of the ring methyl groups attached to the C1 atom with the C8 proton because of an increase in separation of more than  $0.6 \text{ \AA}$ , thereby drastically reducing the violation of van der Waals distances. In both cases the retinal has a 6-*s-trans* as previously found for retinal in bacteriorhodopsin<sup>22</sup> and not the 6-*s-cis* configuration assumed from indirect optical and  $^{13}\text{C}$  NMR chemical shift studies<sup>10, 11, 13, 21</sup>.

In a theoretical calculation of chiro-optical properties for bound 11-*cis* retinal, the observed circular dichroism (CD) spectra show very little dependence on the rotation of the -ionone ring with respect to conjugated polyene chain<sup>11</sup>. The  $^{13}\text{C}$  NMR chemical shift value for the C5 ring atom reported for retinal in rhodopsin is found at the upper end of the region for 6-*s-cis* model compounds, close to the spectral range for 6-*s-trans* compounds. However, the chemical shift value is extremely sensitive to several factors including the degree of conjugation between the C5=C6 double bond and the conjugated bond system of the polyene chain, and the electronic properties of amino-acid residues surrounding the ring moiety. Furthermore, a twist angle of  $70^\circ$  for a 6-*s-trans* configuration of the retinal ring provides a similar degree of conjugational overlap as a ring-chain twist of  $60\text{--}70^\circ$  for a 6-*s-cis* configuration. This situation is very different from the planar 6-*s-trans* retinal model compounds used as references in the NMR studies<sup>21</sup>. Thus, reconciling the structurally and electronically sensitive optical and NMR chemical shift data reported elsewhere<sup>10-14, 21</sup> with the direct and structurally sensitive deuterium NMR presented here, is very difficult.

The average orientation of the retinal axis (defined from C6 to C12) with respect to the membrane plane was found to be  $22^\circ$  from the current study, which is less than the  $32^\circ$  measured by indirect optical (and hence averaged) approaches<sup>10-13</sup>. The rotational angle of  $55^\circ$  for the retinal plane (defined as C6–C9–C19) is slightly larger than the  $40\text{--}50^\circ$  range indicated by optical studies<sup>13</sup>. However, the discrepancies may result simply from the fact that the retinal environment contains a complex electronic

distribution that contributes significantly to measured optical spectra, but does not give direct structural constraints for the individual molecular chromophoric segments separately. These details are, however, available from the electronic-insensitive but structurally sensitive deuterium NMR approach used here.

The position of the chromophore with respect to the membrane bilayer has been resolved (Fig. 3) using information from the helix wheel representation for rhodopsin in the ground state<sup>3</sup>. Here, Lys296 (helix VII:11 in the nomenclature used there<sup>3</sup>) is close to the centre of the membrane, and the -ionone ring of retinal is close to the conserved tryptophan (at VI:16), with the side chain of tyrosine (at VI:19) which is found in all opsins, and the side chain of alanine (or threonine) (VI:20) found in mammalian opsins, below the retinal ring. This indicates that the -ionone ring should point towards the intracellular side of the membrane, as shown here, but this intermolecular information for retinal with respect to the protein is not revealed by the current NMR data for symmetry reasons.

The unique structure of the chromophore reflects the remarkable efficiency of retinal, when located in the binding pocket of rhodopsin, to convert 30–35 kcal/mol of light energy into a chemical signal by undergoing isomerization to an all-*trans* structure<sup>1, 14, 17</sup>. The channelling of this energy to the protein body is thought to provide the main force for protein activation. To determine the orientation and proposed relaxed all-*trans* conformation of the chromophore in the MI-state of the protein, 2H NMR experiments, were carried out on irradiated rhodopsin samples trapped at the MI state. For all C–C(2H) 3 bond vectors, angles between 60° and 65° were obtained (Table 1)

	C <sub>5</sub> –C <sub>18</sub>	C <sub>9</sub> –C <sub>19</sub>	C <sub>13</sub> –C <sub>20</sub>
Dark state	21 ± 5°	44 ± 5°	30 ± 5°
M <sub>i</sub> state	62 ± 7°	65 ± 10°	60 ± 10°

Bond vectors for each of the labelled segments of retinals within bovine rhodopsin measured directly from the <sup>2</sup>H-NMR spectra.

reflecting the relaxed structure of the chromophore in agreement with the recently obtained torsion angle of 180° for the C10–C11

segment<sup>18</sup>, and intraligand distance measurements<sup>17</sup> around this segment confirming a relaxed all-*E* structure. The structure shown in Fig. 3 indicates a combined movement of the ring and the C6–C 11 segment relative to the Schiff base upon activation. The three bond vectors are roughly collinear, so the torsion angle of the chromophore plane relative to the membrane plane can only be accounted for by a tilt of the retinal axis. Using a reasonable value between 30° and 35° for the tilt of the axis (a change of 10° occurs upon activation<sup>13, 14</sup>) a rotation of the chromophore plane through an angle of 45° to 50° occurs upon isomerization.

Deriving structurally relevant information at the atomic level for agonists and antagonists for GPCRs will enable detailed insights into their binding and activation, as shown here on the photo-receptor protein bovine rhodopsin. The structural information obtained allows a critical evaluation of binding sites and binding modes of GPCR ligands, particularly with respect to recent assumptions about the existence of a binding pocket within the transmembrane domain which may be highly conserved throughout the whole family of GPCRs<sup>3-6, 8</sup>. To define this structural feature of receptor activation is not only important for rhodopsin related diseases, but is of general relevance to the activation of the large family seven transmembrane domain GPCRs that rely on diffusing transmitter molecules.

## Methods

**Sample preparation** Three different retinals were synthesized<sup>7, 19</sup>, all analogues of the naturally occurring chromophore but with each of the following methyl groups, C5–C18, C9–C19 and C13–C20, carrying deuterium C–C(2H)<sub>3</sub>. Rhodopsin was isolated from bovine retina but with its indigenous retinal removed to give chromophore-free opsin<sup>17, 19</sup>. Each of the labelled retinals was introduced into the opsin to give a fully functional rhodopsin which is embedded in bilayers using well established methods<sup>19, 20</sup>.

**NMR experiments** NMR experiments were carried out at 61.402 MHz on a BRUKER MSL 400 using a 7-mm MAS probe. Spectra were recorded using a 'single pulse' sequence with the sample subject to MAS. The pulse length was typically 5  $\mu$ s. The spinning rate was stabilized to about 3 kHz. Measurements were performed at 213 K using a spinning speed of 2860 Hz, a recycle delay of 300  $\mu$ s and around 400,000 scans. Spectra were processed with 16 K zerofilling applying 100 Hz of exponential line broadening.

**Data analysis** The symmetrized NMR spectra were analysed using a program for MAS lineshape simulations of oriented systems based on the NMR software library GAMMA as described<sup>7</sup>. The observed MAS sideband distribution depends on the tilt angle  $\theta$  of the C–C(2H)<sub>3</sub> bond vector with respect to the protein long axis ZM, defined by the orientation of helix 7. The distribution of ZM about the sample director ZD, which is caused by some remaining disorder in the sample is described by a three-dimensional Gaussian distribution of the spectral width. A spectral deconvolution analysis applied to spectrum of [Fig. 2b](#) showed that more than 80% of the sample was in the MI state.

To relate the orientational constraints obtained by the simulation package (obtained with respect to the membrane normal) to the protein body itself, a protein reference system was chosen based on the latest structure<sup>2</sup> for the arrangement and positions of the seven transmembrane helices in bovine rhodopsin in the ground state. The projection maps reveal helix 7, where 11-*cis* retinal is attached to the  $\epsilon$ -amino group of Lys<sup>296</sup>, as collinear with the membrane normal, and therefore helix 7 has been used here as representative of the protein long axis ZM ([Fig. 3](#)).

Received 20 October 1999; accepted 17 March 2000

## References

1. Birge, R. R. Nature of the primary photochemical events in rhodopsin and bacteriorhodopsin. *Biochim. Biophys. Acta* **1016**, 293-327 (1990). [Article](#) [PubMed](#) [ISI](#) [ChemPort](#)
2. Krebs, A., Villa, C., Edwards, P. C. & Schertler, G. F. X. Characterisation of an improved two-dimensional p22121 crystal from bovine rhodopsin. *J. Mol. Biol.* **282**, 991-1003 (1998). [Article](#) [PubMed](#) [ISI](#) [ChemPort](#)

3. Baldwin, J. M., Schertler, G. F. X. & Unger, V. M. An alpha-carbon template for the transmembrane helices in the rhodopsin family of G-protein-coupled receptors. *J. Mol. Biol.* **272**, 144-164 (1997). [Article](#) [PubMed](#) [ISI](#) [ChemPort](#)
4. Baldwin, J. M. Structure and function of receptors coupled to G proteins. *Curr. Opin. Cell Biol.* **6**, 180-190 (1994). [PubMed](#) [ISI](#) [ChemPort](#)
5. Donnelly, D. & Findlay, J. B. C. Seven-helix receptors: structure and modelling. *Curr. Opin. Struct. Biol.* **4**, 582-589 (1994). [ISI](#) [ChemPort](#)
6. Herzyk, P. & Hubbard, R. E. Combined biophysical and biochemical information confirms arrangement of transmembrane helices visible from the three-dimensional map of frog rhodopsin. *J. Mol. Biol.* **281**, 741-754 (1998). [Article](#) [PubMed](#) [ISI](#) [ChemPort](#)
7. Glaubitz, C., Burnett, I. J., Gröbner, G., Mason, A. J. & Watts, A. Deuterium-MAS NMR spectroscopy on oriented membrane proteins: applications to photointermediates of bacteriorhodopsin. *J. Am. Chem. Soc.* **121**, 5787 (1999). [Article](#) [ISI](#) [ChemPort](#)
8. Ji, T. H., Grossmann, M. & Ji, I. G Protein-coupled receptors. *J. Biol. Chem.* **273**, 17299-17302 (1998). [Article](#) [PubMed](#) [ISI](#) [ChemPort](#)
9. Altenbach, C., Cai, K., Khorana, H. G. & Hubbell, W. L. Structural features and light-dependent changes in the sequence 306-322 extending from helix VII to the palmitoylation sites in rhodopsin: a site-directed spin-labeling study. *Biochemistry* **38**, 7931-7937 (1999). [Article](#) [PubMed](#) [ISI](#) [ChemPort](#)
10. Tan, Q. *et al.* Absolute sense of twist of the C12-C13 bond of the retinal chromophore in bovine rhodopsin based on exciton-coupled CD spectra of 11,12-dihydroretinal analogues. *Angew. Chem Int. Ed.* **36**, 2089-2093 (1997). [ISI](#) [ChemPort](#)
11. Buss, V., Kolster, K., Terstegen, F. & Vahrenhorst, R. Absolute sense of twist of the C12-C13 bond of the retinal chromophore in rhodopsin-semiempirical and nonempirical calculations of chiroptical data. *Angew. Chem Int. Ed.* **37**, 1893-1895 (1998). [Article](#) [ISI](#) [ChemPort](#)
12. Rothschild, K. J., Sanches, R., Hsiao, T. L. & Clark, N. A. A spectroscopic study of rhodopsin alpha-helix orientation. *Biophys. J.* **31**, 53-64 (1980). [PubMed](#) [ISI](#) [ChemPort](#)
13. Jaeger, S. *et al.* Chromophore structural changes in rhodopsin form nanoseconds to microseconds following pigment photolysis. *Proc. Natl Acad. Sci. USA* **94**, 8557-8562 (1997). [Article](#) [PubMed](#)
14. Shieh, T., Han, M., Sakmar, T. P. & Smith, S. O. The steric trigger in rhodopsin activation. *J. Mol. Biol.* **269**, 373-384 (1997). [Article](#) [PubMed](#) [ISI](#) [ChemPort](#)
15. Eilers, M., Reeves, P. J., Ying, W., Khorana, H. G. & Smith, S. O. Magic angle spinning NMR of the protonated retinylidene Schiff base nitrogen in rhodopsin: Expression of <sup>15</sup>N-lysine- and <sup>13</sup>C-glycine-labeled opsin in a stable cell line. *Proc. Natl Acad. Sci. USA* **96**, 487-492 (1999). [Article](#) [PubMed](#) [ISI](#) [ChemPort](#)
16. Feng, X. *et al.* Direct determination of a molecular torsional angle in the membrane protein rhodopsin by solid-state NMR. *J. Am. Chem. Soc.* **119**, 6853-6857 (1997). [Article](#) [ISI](#) [ChemPort](#)
17. Verdegem, P. J. E. *et al.* Retinylidene ligand structure in bovine rhodopsin, metarhodopsin-I, and 10-methylrhodopsin from internuclear distance measurements using <sup>13</sup>C-labeling and 1D rotational resonance MAS NMR. *Biochemistry* **33**, 11316-11324 (1999). [Article](#) [ChemPort](#)
18. Feng, X. *et al.* Determination of a molecular torsional angle in the metarhodopsin-I photointermediate of rhodopsin by double-quantum solid-state NMR. *J. Biomol. NMR* **16**, 1-8 (2000). [Article](#) [PubMed](#) [ISI](#) [ChemPort](#)

19. Gröbner, G. *et al.* Photoreceptor rhodopsin: structural and conformational study of its chromophore 11-cis retinal in oriented membranes by deuterium solid state NMR. *FEBS Lett.* **422**, 201-204 (1998). [Article](#) [PubMed](#) [ISI](#)
20. Gröbner, G. *et al.* Macroscopic orientation of natural and model membranes for structural studies. *Anal. Biochem.* **254**, 132-138 (1997). [Article](#) [PubMed](#) [ISI](#)
21. Smith, S. O. *et al.* Low-temperature solid-state <sup>13</sup>C NMR studies of the retinal chromophore in rhodopsin. *Biochemistry* **26**, 1606-1611 (1987). [PubMed](#) [ISI](#) [ChemPort](#)
22. Hudson, B. S. & Birge, R. R. Angular orientation of the retinyl chromophore of bacteriorhodopsin: Reconciliation of <sup>2</sup>H NMR and optical measurements. *J. Phys. Chem. A* **103**, 2274-2281 (1999). [Article](#) [ISI](#) [ChemPort](#)

**Acknowledgements.** We thank P. Fisher and B. Bonev for help, and J. Lugtenburg for discussion and advice. This work was supported by grants to A.W. (MRC, BBSRC, EU TMR, EU Biotech, Magnex, Varian, Bruker and HEFCE); C.G. is supported by a DFG Emmy Noether Fellowship.

-----